High-Pressure–High-Temperature Study of Spin-Lattice Relaxation in Pure and Doped LiBr Single Crystals*†

K. LINGA MURTY‡ AND ARTHUR L. RUOFF
Department of Applied Physics and Materials Science and Engineering, Cornell University, Ithaca, New York 14850
(Received 28 July 1969)

Measurements of the spin-lattice relaxation time of Li in pure and doped single crystals of LiBr, as a function of temperature, clearly indicate that the spin relaxation is due predominantly to the diffusive motion above room temperature. The magnitude and temperature dependence of the relaxation time and the magnitude of temperature at which $T_{1\min}$ occurs favor Torrey's theory of dipolar relaxation due to translational diffusion of Li^+ ions over Reif's quadrupolar mechanism due to vacancy diffusion. The study of temperature dependence facilitated a determination of activation energies for creation and motion of vacancies in this material. The low-temperature slopes of the normalized frequency y $(=\omega_0/2\nu)$ versus $1/kT$ curves yielded a value of 0.35 eV corresponding to the activation energy for motion of a vacancy. The high-temperature slope fixed the value of the activation energy of formation of a Schottky pair at 1.70 eV. These values are in essential agreement with those obtained from ionic conductivity measurements. The effect of pressure on longitudinal relaxation time at temperatures ranging from room temperature to about 400°C was investigated up to about 5 kbar. The activation volume for the motion of a vacancy was found to be 6.4 cm^3/mole. The study of pressure dependence at high temperatures gave a value of 29.5 cm^3/mole for the formation volume of a Schottky-pair defect. These values of the activation volumes are comparable to the previous determinations in other alkali halides by ionic conductivity studies and are also in reasonable agreement with those predicted by Keyes's strain-energy model.

I. INTRODUCTION

NUCLEAR magnetic resonance (NMR) is one of the most powerful techniques employed to study diffusion in solids. The profound effect of diffusion on NMR had been recognized even at the time of the first discovery.[1] The relaxation of a nucleus is affected by the relative motions of nearby nuclei. The relaxation times in these cases depend directly on the rate of atom jumping, in contrast to ionic conductivity or radioactive tracer diffusion experiments where the net transport effect of diffusion is observed. Thus, in principle, one could get a better microscopic picture of the diffusion process by NMR techniques. The importance of NMR in the study of imperfections in solids, particularly ionic crystals, has been demonstrated by Reif.[2] His work revealed that by careful studies in these solids by NMR techniques, one should be able to determine various diffusion parameters accurately. However, many different mechanisms may be operative over the same temperature range and it is not always possible to separate them. The amount of diffusion information obtainable may be greatly restricted if a diffusion-independent mechanism predominates over a large temperature range.[3,4] In general, this situation prevails in solids consisting of nuclei with large quadrupole moments. This was clearly demonstrated for Na in NaF,[5] for Na and I in NaI,[6] and for Br in LiBr.[7]

Holcomb and Norberg[8] successfully made diffusion studies in metallic lithium and sodium by NMR techniques. Spokas and Slichter's work on aluminum,[3] at a later date, revealed the importance of NMR in the determination of diffusion parameters. Hultsch and Barnes[9] extended Holcomb and Norberg's work by studying the pressure dependence of spin relaxation in lithium and sodium.

The study of Allen and Weber[7] on lithium in LiBr revealed that the spin-lattice relaxation of the lithium nucleus is due mainly to diffusion above room temperature and also that an accurate quantitative determination of diffusion parameters is possible in this case. An obvious extension of their investigation is to work with LiBr single crystals doped with a divalent impurity, thereby creating mobile Li^+ vacancies. In the temperature region where spin relaxation is controlled by a diffusion process, a study of pressure dependence of the relaxation should enable one to determine activation parameters such as the activation volumes for motion and creation of vacancies. Combined with temperature measurements, the enthalpy $H=E+PV$ for the particular diffusion process can be obtained. Thus, in the present work, NMR pulse techniques were employed to measure the spin-lattice relaxation time of lithium in pure and doped LiBr single crystals as a function of temperature (from 300 to about 750°K) and

* Based on a thesis submitted by K. L. Murty to the Faculty of the Graduate School of Cornell University in partial fulfillment of the requirements for the Ph.D. degree.

† Supported by the Atomic Energy Commission and also by the Advanced Research Projects Agency through the facilities of the Materials Science Center at Cornell University.

‡ Present address: Laboratory for Crystallographic Research, Department of Physics and Astronomy, Rensselaer Polytechnic Institute, Troy, N. Y.

[1] N. Bloembergen, E. M. Purcell, and R. V. Pound, Phys. Rev. **73**, 679 (1948).
[2] F. Reif, Phys. Rev. **100**, 1597 (1955).
[3] J. J. Spokas and C. P. Slichter, Phys. Rev. **113**, 1462 (1958).
[4] F. Tuler, Ph.D. thesis, Cornell University, 1967 (unpublished).
[5] P. P. Mahendroo and A. W. Nolle, Phys. Rev. **126**, 125 (1962).
[6] W. G. Clark, Ph.D. thesis, Cornell University, 1961 (unpublished).
[7] R. R. Allen and M. J. Weber, J. Chem. Phys. **38**, 2970 (1963).
[8] D. F. Holcomb and R. E. Norberg, Phys. Rev. **98**, 1074 (1954).
[9] R. A. Hultsch and R. G. Barnes, Phys. Rev. **125**, 1832 (1961).

pressure (up to 5 kbar in the temperature range from 300 to about 673°K).

II. THEORY

A. Spin-Lattice Relaxation

A number of relaxation processes are possible in a solid and each relaxation mechanism is characterized by a specific temperature dependence. Thus a study of the temperature dependence of the spin-lattice relaxation time T_1 serves to show which mechanisms are operative. Mahendroo and Nolle[5] summarized possible mechanisms—dipolar and quadrupolar—in solids, particularly ionic crystals. In the case of nuclei with a quadrupole moment (i.e., $I>\frac{1}{2}$), either the spin-lattice relaxation due to lattice phonons or the relaxation limited by spin-spin diffusion to paramagnetic impurities is important at sufficiently low temperatures, while for nuclear spins equal to $\frac{1}{2}$ the nuclear magnetic relaxation at low temperatures is always caused by the interaction of the nuclear spins with the spins of paramagnetic impurities.[10] At sufficiently high temperatures, however, the relaxation proceeds through diffusive motions of the nuclei or the point defects such as charged vacancies or interstitials. In the event that quadrupolar interactions are weak, the spin-lattice relaxation at high temperatures is usually due to dipole-dipole interactions via the diffusional motion of the nuclei. If strong quadrupolar interactions are present, such as in ionic crystals, the motion of imperfections in the lattice creates fluctuating electric field gradients at the position of the nucleus and may constitute an important relaxation mechanism for the nucleus through interaction with its quadrupole moment. This relaxation via diffusional motion is ineffective in the regions where diffusion is slow. As the temperature increases, diffusion becomes more rapid and the transition probability increases. This process reaches its peak effectiveness when the diffusion jump frequency is in the neighborhood of the nuclear Larmor frequency.

A theory of the spin-lattice relaxation due to the interactions of the nuclei with fluctuating local magnetic fields has been given by Bloembergen, Purcell, and Pound.[1] Their theory was developed for isotropic liquid media and here the diffusion coefficient enters just as a parameter, while, in principle, nuclear-spin relaxation should provide a means of studying the diffusion process from a microscopic point of view. Torrey[11] has extended the above theory, treating the problem by the theory of random walk. He studied specific cases of translational lattice diffusion. Torrey's calculations were reevaluated later by Resing and Torrey[12] using the revised theoretical expression for T_1 of Kubo and Tomita. They obtain, for the relaxation rate, the expression

$$\frac{1}{T_1}=\frac{\gamma^4\hbar^2 I(I+1)8\pi nc}{3k^3l^3\omega_0}\psi(k,y)\,, \tag{1}$$

where γ is the gyromagnetic ratio of the nucleus, I is the nuclear spin in units of $\hbar$, $n=c/2R_0^3$ is the spin density, with R_0 being the nearest-neighbor distance, c is the ratio of the number of nuclei to that of lattice sites ($\simeq 1$), $k=a/l$, where a is the closest possible distance of approach of two nuclei and l is the jump distance, ω_0 is the Larmor frequency, and

$$\psi(k,y)=yG(k,y)+4yG(k,2y)\,,$$

where $y=\omega_0/2\nu$, ν is the jump frequency, and G is a complicated integral given by Torrey.[11] Resing and Torrey[12] tabulated $\psi(k,y)$ for various values of y and found that $\psi_{\max}=0.4387$ when $y=0.55$ for $k=0.7428$, corresponding to an fcc lattice.

Quadrupolar relaxation by the diffusional motion of defects is discussed by Cohen and Reif[13] and by Reif.[2] Reif treated this problem of relaxation through single-phonon processes produced by the diffusion of lattice vacancies. He adapted Torrey's theory of relaxation due to translational diffusion in a lattice to obtain[2]

$$\frac{1}{T_1}=\frac{16\pi}{45}(1+k')Bc\nu\frac{\omega_0}{\nu^2+\frac{5}{2}(1+k')^2\omega_0^2}\,, \tag{2}$$

where $1+k'$ is 1.116 for vacancies restricted to sites of ions, unlike the one undergoing relaxation in an alkali-halide lattice, or is 1.3125 for the case of like sites. c is the vacancy concentration, ν is the vacancy jump frequency, and

$$B=\frac{9(2I+3)}{64I^2(2I-1)\omega_0}\left(\beta\frac{e^2Q}{\hbar R^3}\right)^2\,, \tag{3}$$

where β is the effective antishielding factor, e is the electron charge, Q is the quadrupole moment of the nucleus, and R is the nearest-neighbor distance. In obtaining the above expression, Reif used the approximate evaluation of the Torrey integrals which is valid for $k>\frac{1}{2}$. It is clear from the above expression for T_1 that the characteristic minimum in T_1 is reached when $\nu\approx(\frac{5}{2})^{1/2}(1+k')\omega_0$. It is to be noted that while at low temperatures c is determined by the concentration of divalent impurities, at high enough temperatures c increases with temperature due to the generation of thermal vacancies, and as a result $1/T_1$ will tend to increase again. We will come back to this point later.

[10] G. R. Khutsishvili, Zh. Eksperim. i Teor. Fiz. **31**, 424 (1956) [English transl.: Soviet Phys.—JETP 4, 382 (1957)].
[11] H. C. Torrey, Phys. Rev. **92**, 962 (1953).
[12] H. A. Resing and H. C. Torrey, Phys. Rev. **131**, 1102 (1963).
[13] M. H. Cohen and F. Reif, in *Solid State Physics*, edited by F. Seitz and D. Turnbull (Academic Press Inc., New York, 1957), Vol. 5.

B. Activation Parameters and Spin-Lattice Relaxation Time

The vacancy jump frequency ν can in general be written as

$$\nu=\nu_0 e^{-G_m/RT}, \tag{4}$$

where $G_m=H_m-TS_m$ is the Gibbs free energy of motion of a vacancy and ν_0 is a frequency factor of the order of 10^{13} sec^{-1}. The activation enthalpy for the motion of a vacancy $H_m=E_m+PV_m$ can be obtained from the temperature dependence of ν:

$$H_m=-R\left[\frac{\partial \ln\nu}{\partial(1/T)}\right]_P, \tag{5}$$

where the subscript P indicates differentiation at constant pressure. Similarly, the pressure dependence of ν permits a determination of the activation volume for motion of a vacancy:

$$V_m=-RT\left(\frac{\partial \ln\nu}{\partial P}\right)_T. \tag{6}$$

In the present case of ionic crystals the positive vacancy concentration c at low temperatures is primarily due to the divalent impurity content and is thus temperature-independent. However, at higher temperatures thermal vacancies dominate and c can then be written as

$$c=c_0 e^{-G_f/2RT}, \tag{7}$$

where $G_f=E_f+PV_f-TS_f$ is the change in Gibbs's free energy required to form a Schottky pair.

Now, to relate the above activation parameters to the spin-lattice relaxation time we consider the two regions, extrinsic and intrinsic, separately.

In the extrinsic region the vacancy concentration c can be taken as a constant determined essentially by the divalent impurity content. Torrey's expression for T_1 [Eq. (1)] gives, at low temperatures,

$$T_1=N2\omega_0^2a^6/\nu_{\mathrm{Li}}, \quad \omega_0\tau\gg 1 \tag{8}$$

where N is a constant with factors independent of temperature and pressure, a is the lattice parameter, τ is the jump correlation time, and ν_{Li} is the jump frequency of a lithium nucleus given by $\nu_{\mathrm{Li}}=zc\nu$, i.e., ν times the probability that a nearest-neighbor positive-ion site is vacant. Here z is the number of nearest-neighbor cation sites in a NaCl-type lattice. Writing ν explicitly, we find that

$$T_1\propto(\omega_0^2a^6/c\nu_0)e^{G_m/RT},$$

so that

$$H_m=R\left[\frac{\partial \ln T_1}{\partial(1/T)}-6\frac{\partial \ln a}{\partial(1/T)}\right]_P$$

and

$$V_m=RT\left[\frac{\partial \ln T_1}{\partial P}+\frac{\partial \ln\nu_0}{\partial P}-6\frac{\partial \ln a}{\partial P}\right]_T. \tag{9}$$

In the Reif treatment we find that $T_1\propto\omega_0a^6/c\nu$, so that here also the above equations are valid.

At higher temperatures but still in the extrinsic region the jump correlation time decreases and the Torrey theory shows that

$$T_1=\tfrac{1}{2}N\nu_{\mathrm{Li}}a^6, \quad \omega_0\tau\ll 1 \tag{10}$$

where N is the same constant factor as in the earlier case. One thus obtains, in this region,

$$H_m=-R\left[\frac{\partial \ln T_1}{\partial(1/T)}-6\frac{\partial \ln a}{\partial(1/T)}\right]_P$$

and

$$V_m=RT\left[-\frac{\partial \ln T_1}{\partial P}+\frac{\partial \ln\nu_0}{\partial P}+6\frac{\partial \ln a}{\partial P}\right]_T. \tag{11}$$

Reif predicts that in the region where $\omega_0\ll\nu$, $T_1\propto(\nu/c)a^6$, so that here again, the above equations are valid.

However, at still higher temperatures intrinsic vacancies overtake the extrinsic and the change in Gibbs's free energy for formation of vacancies should come into the picture. In such a case, in the intrinsic region and in the region where $\omega_0\tau\ll 1$ holds, Torrey's theory yields

$$T_1=\tfrac{1}{2}Na^6\nu_0c_0e^{-(\frac{1}{2}G_f+G_m)/RT}.$$

Thus

$$\tfrac{1}{2}H_f+H_m=-R\left[\frac{\partial \ln T_1}{\partial(1/T)}-6\frac{\partial \ln a}{\partial(1/T)}\right]_P$$

and

$$\tfrac{1}{2}V_f+V_m=RT\left[-\frac{\partial \ln T_1}{\partial P}+\frac{\partial \ln\nu_0}{\partial P}+6\frac{\partial \ln a}{\partial P}\right]_T. \tag{12}$$

However, the Reif mechanism predicts, in this case, that

$$T_1\propto(\nu/c)a^6\sim(\nu_0/c_0)a^6e^{(\frac{1}{2}G_f-G_m)/RT},$$

so that

$$R\left[\frac{\partial \ln T_1}{\partial(1/T)}-6\frac{\partial \ln a}{\partial(1/T)}\right]_P=\tfrac{1}{2}H_f-H_m$$

and

$$RT\left[\frac{\partial \ln T_1}{\partial P}-\frac{\partial \ln\nu_0}{\partial P}-6\frac{\partial \ln a}{\partial P}\right]_T=\tfrac{1}{2}V_f-V_m. \tag{13}$$

Thus we note that the temperature dependence of T_1 is different for the two treatments considered above: Reif's analysis through vacancy diffusion and Torrey's treatment based on the lithium-ion jumping. In the present experiments, the Larmor frequency is such that the condition $\omega_0\ll\nu$ is achieved before the thermal vacancies gain importance over the extrinsic vacancies. This primarily is the reason to assume, in the above analysis, that the criterion $\omega_0\tau\ll 1$ is valid in the intrinsic region.

III. EXPERIMENTAL DETAILS

A. NMR Spectrometer

The measurement of relaxation times was carried out on a phase-coherent pulsed NMR spectrometer of a design originally made by Clark.[14] The NMR apparatus of this study is a slightly modified version of that of Tuler,[4] who used it for an investigation of pressure dependence of spin relaxation in aluminum. Both double- and single-coil versions were used. Although there is not much to choose between the two as far as signal-to-noise ratio is concerned, the single-coil configuration has the advantage of extreme simplicity. The spectrometer consists of a continuously running 5.5-Mc/sec crystal oscillator which provides a reference signal to the receiver and the radio frequency for the transmitter pulses. The nuclear signal is picked up by an rf preamplifier which is a replica of Clark's.[14] The required optimization in the transmitting and the receiving modes, in the case of a single-coil arrangement, was achieved using the circuit described by Gray *et al.*[15] The signal goes from the preamplifier into the receiver, an Arenberg WA-600-D wide-band amplifier. The signal is thus amplified 10^4 times and is displayed after detection on a Tektronix 564 storage oscilloscope. The data were recorded on Polaroid 3000 speed film. The reciver recovery time was minimized by connecting back-to-back diodes at the input to the preamplifier and a dead time of about 20 μsec was considered tolerable.

B. Probes

The transmitter coil form of the double-coil arrangement was made out of Lava A (from American Lava Co., Chattanooga, Tenn). The receiver coil form was an ampule that served as the sample holder and was machined either of boron nitride or Alsimag 222 (also American Lava Co.). The transmitter coil was wound with 0.025-in. gold wire and the receiver coil with 0.010-in. gold wire in the machined threads on the forms. The coil form of the single-coil configuration was machined of Alsimag 222 and $\sim$0.02-in. gold wire was used for the coil wire.

C. Heater and Temperature Control

The heater consisted of 0.01-in. Nichrome wire wound back and forth noninductively through $\frac{1}{16}$-in.-diam$\times$1-in. pieces of alumina tubing. These pieces of alumina tubing, as long as the ampule and standing side by side, completely encircled the receiver coil. Thus the heater, the receiver coil, and the ampule assembly fitted snugly in the transmitter coil form. In the case of the single-coil configuration, the heater encircled the sample and the heater-sample assembly snugly fitted into the coil form.

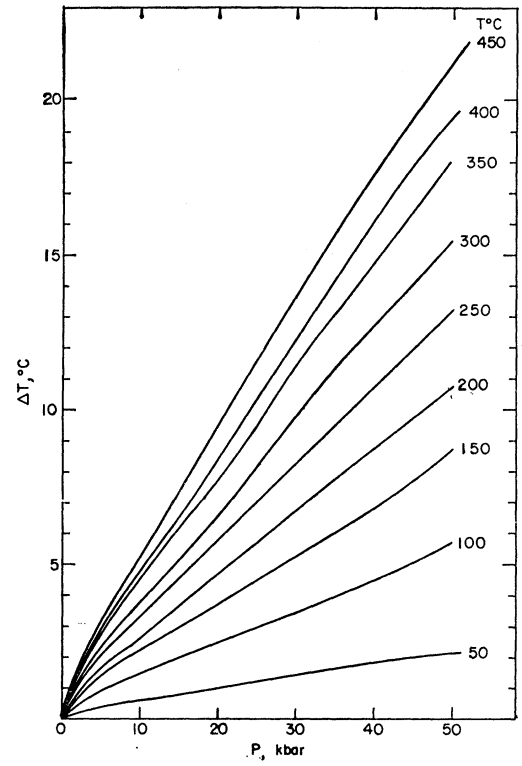

FIG. 1. ΔT as a function of pressure at various temperatures obtained from isothermal cuts of the data in Ref. 16.

A Pt-(Pt 10% RH) thermocouple was inserted in the heater windings in the double-coil arrangement. It was placed in between the sample and the heater, touching both, in the case of the single-coil configuration. The temperature was controlled by a Honeywell proportional controller. Either a Honeywell set point unit or a Leeds and Northrup K-3 potentiometer was used to measure the temperature. Thus it has been possible to control the temperature to better than ± 0.1°C below about 400°C, while at higher temperatures the error could be as large as 1°C.

The emf of the thermocouple is known to be a function of pressure and the measured temperatures were corrected through the relationship

$$T_{\text{corr}} = T_{\text{meas}} + \Delta T.$$

Hanneman and Strong[16] gave ΔT as a function of temperature at various pressures. Figure 1 shows ΔT as a function of pressure at various temperatures of interest here, obtained from isothermal cuts of their data. Thus in the present work the pressure dependence was studied at constant thermo-emf of the thermocouples and in actuality no isothermal data could be obtained.

[14] W. G. Clark, Rev. Sci. Instr. **35**, 316 (1964).

[15] K. W. Gray, W. N. Hardy, and J. D. Noble, Rev. Sci. Instr. **37**, 587 (1966).

[16] R. E. Hanneman and H. M. Strong, J. Appl. Phys. **36**, 523 (1965).

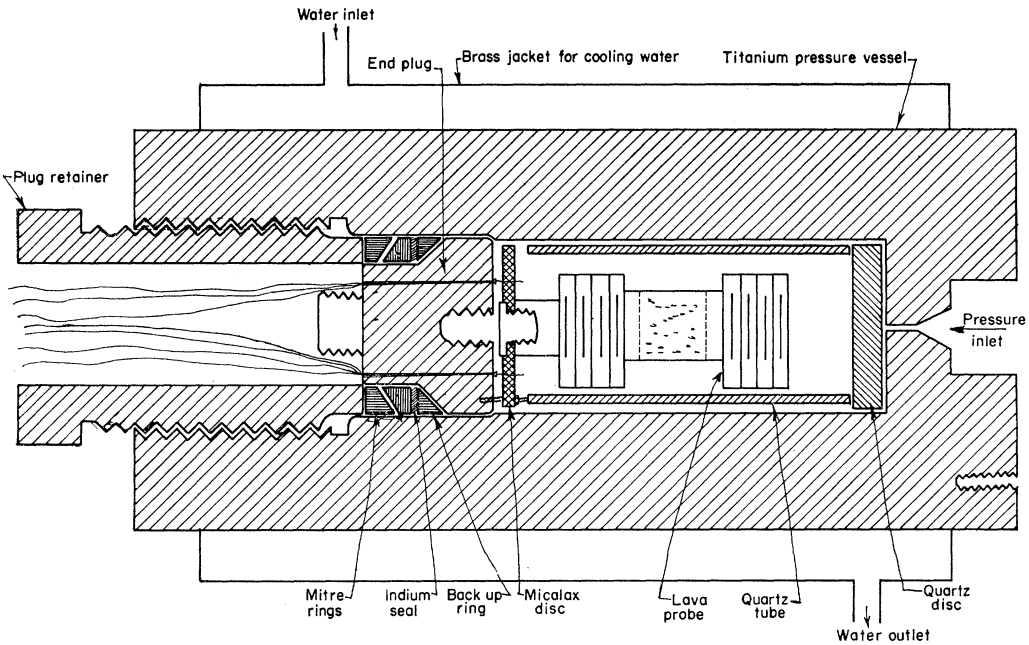

FIG. 2. Cross section of the pressure vessel with the probe assembly.

D. High-Pressure System

The pressure was generated using a Haskel air-driven hydraulic pump rated with a maximum output pressure of 75 000-psi at 120-psi input air pressure. Bourdon tube gauges were used as pressure-measuring devices, and the pressure was transmitted from the high-pressure generator to the gauge and pressure vessel through standard $\frac{5}{16}$-in.-o.d.$\times\frac{1}{16}$-in.-i.d. 316 stainless high-pressure fittings and valves. Three centistokes Dow Corning 200 silicone fluid was used as the pressure-transmitting medium for the temperatures and pressures of this investigation. The accuracy in the measurement of pressure is better than ± 100 psi ($=\pm 7$ bar).

Figure 2 shows a cross section of the pressure vessel with the probe assembly. The pressure vessel was made of Crucible C-130AM titanium base alloy. The tensile properties of this alloy decrease with temperature and so it is necessary to keep it cool with circulating cold water. The pressure fluid enters the vessel from right (Fig. 2) through a $\frac{5}{16}$-in. 316 stainless-steel tubing, and the gland nut and the high-pressure fitting were made of 304 stainless steel. High-pressure sealing was achieved through a Bridgmann unsupported-area-type indium seal. The end plug made of the same titanium alloy was backed up by a titanium backup ring, indium ring, and two titanium mitre rings, in that order. All this assembly of the end plug, backup ring, indium seal, and the mitre rings were retained by a titanium plug retainer.

All the seven leads—two for the receiver, one for the transmitter (the other lead was grounded to the end plug), two for the heater, and two for the thermocouple—entered through the seven holes symmetrically drilled in the end plug. Brass cones were used for pressure sealing and these were insulated from the plug by Kynar (thermofit) sleevelets. All the cones had holes drilled all the way through and were silver-soldered to the wires. Thus it had been possible to eliminate a probable emf source at the cone connections for the thermocouple leads. All eight leads were rigidly placed and insulated by passing them through alumina tubing cemented to the probe with Saureisen cement. Excepting the thermocouple leads, copper wires were fed through the cones and these were silver-soldered at the probe end of the end plug to the respective leads, either gold or Nichrome.

To minimize heater losses due to convection currents, a quartz tube 1.75 in. o.d.$\times\sim 4$ in. long, which fits around the probe and into the bore of the pressure vessel and long enough to reach from the end plug to the other end of the vessel, was inserted in the bomb. Quartz or Micolax disks about $\frac{5}{16}$ in. thick and of roughly the same diameter as the inside diameter of the pressure vessel (Fig. 2) were fixed to each end of the probe to minimize end losses.

E. Samples

Lithium-bromide powder was obtained from two sources: (i) K and K Chemical Co., Long Island, N. Y., and (ii) Merck Ag, Karlsruho, Germany. The material supplied by the above two sources was not of required purity and it was necessary to purify the powder before growing the crystal. As-received powder was baked in a vacuum of about 10^{-5} Torr at 300°C for about 3 days while very slowly increasing and decreasing the tem-

perature. To avoid any contamination, platinum crucibles were used. The material received from the first source had still to be purified and further purification was achieved by melting the powder in a platinum crucible and pumping high-purity bromine gas into the melt for several hours. The crystals were grown from purified melt by the Kyropoules technique using pure argon as a protective atmosphere. Doped crystals were grown by adding known amounts of $CaBr_2$ to the lithium-bromide melt. All the crystals of this study are (100) oriented.

A crystal about 4 in. long and roughly of cylindrical shape ($\sim$1 in. in diameter) was first grown. Only a few parts of the crystal were optically pure and these pure pieces were cleaved while the rest of the crystal was unused. These crystals are highly hygroscopic and very brittle. By polishing these crystals on a wet cloth it was possible to obtain crystals $\frac{1}{2}$ in. in diam$\times\frac{3}{4}$ in. in length which fit snugly into the ampule around which the receiver coil was wound. Originally it was thought advantageous to wind the receiver coil directly on the crystal, but it was not feasible to cut grooves on these crystals.

No special effort was devoted to control the impurity concentration of the doped crystals and a gradient, along the length of the 4-in. crystal, of the concentration of Ca impurity was found. Thus different pieces of the same crystal had different concentrations, and these were identified with numbers, while the original crystals were denoted by letters: P, undoped; A, 0.02% $CaBr_2$; B, 0.1% $CaBr_2$; and C, 0.5% $CaBr_2$.

F. Measurement of T_1

At least three different methods were employed in this study depending on the magnitude of T_1 and the feasibility of the method. For T_1 measurements exceeding 1 sec, the picket 90° pulse method otherwise known as the saturation method was employed. The initial saturation in this case is produced by a series of approximately 90° pulses occurring in rapid succession, separated from one another by a time greater than T_2 and much shorter than T_1. The standard two-pulse method is convenient for T_1 shorter than 1 sec, and 180°-90° sequence was preferred to 90°-90° because the change of sign of the free-precession signal associated with the former effectively improved the signal to noise. In order to improve the accuracy, the measurement was also made with 90°-90° series followed about 2 msec later by a third pulse of appropriate angle.[17] The phase angle of the third pulse was such that an echo was observed after the fixed time of 2 msec from the third pulse. The amplitude of the echo is a measure of the free-induction decay signal amplitude following the second pulse. Here again the 180°-(90°$-\theta$) sequence was preferred to 90°-(90°$-\theta$). The quantity $S(\infty)-S(t)$ was plotted as a function of time t on a semilog graph, the slope of which gave T_1^{-1}. Here S is the amplitude either of the free-precession signal or of the echo and was directly read from the polaroid pictures. For each measurement of T_1, 10–20 points were obtained and $S(\infty)-S(t)$ versus t data were fitted by the method of least squares. On this basis, most T_1 measurements were better than $\pm 3\%$, while occasionally measurements of less accuracy were also recorded. At each temperature, 2–5 pressure points were obtained, except for a couple of cases where only one datum was taken, and 2–3 determinations were made at every temperature and pressure.

[17] R. C. Wayne, Ph.D. thesis, Cornell University, 1966 (unpublished).

IV. RESULTS

A. Temperature Dependence—Identification of Relaxation Mechanism

The first objective is to study T_1 as a function of temperature for comparison with the data of Allen and Weber. This study should facilitate identification of the dominant relaxation mechanism. To this effect, and to correlate the experimental results with predictions of various theories, we concentrate on the $T_1(T)$ data obtained on sample B with 4.4×10^{-4} M concentration of calcium. Figure 3 is a plot of spin-lattice relaxation time as a function of temperature of Li^7 in this sample. Results obtained with different methods are explicitly shown to give an example of typical experimental data. The effect of divalent impurity on T_1 can be seen in the

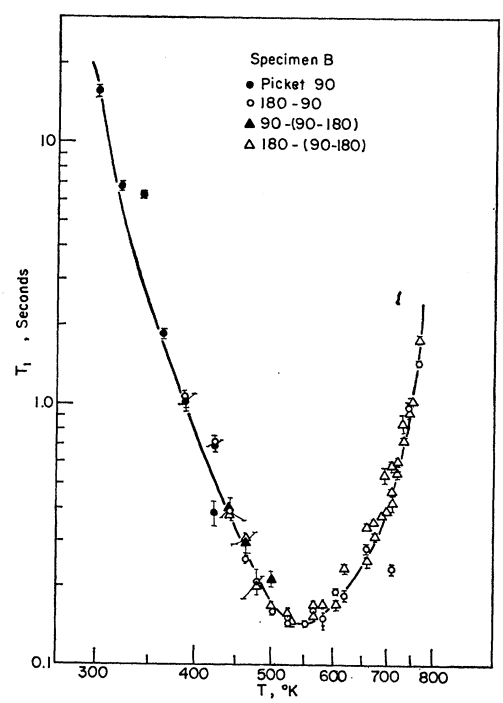

FIG. 3. Spin-lattice relaxation time as a function of temperature in sample B.

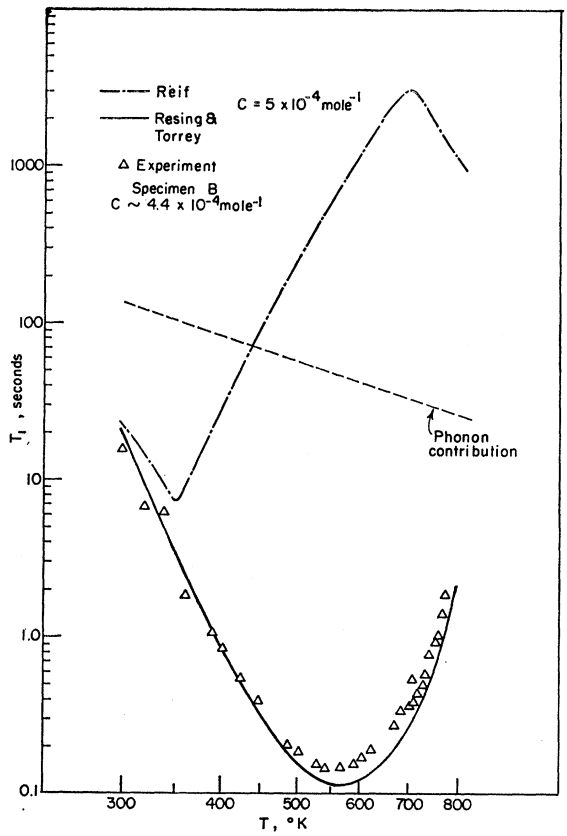

FIG. 4. $T_1(T)$ as calculated from Torrey and Reif theories and as obtained from experiments on sample B. The phonon contribution $\sim T^{-2}$, calculated from Br^{81} data of Ref. 7 is also included.

inset of Fig. 5, where at temperatures below $T_{1\,\mathrm{min}}$, the relaxation time decreases as the impurity concentration increases. The fact that even at room temperature T_1 depends on the impurity concentration indicates that diffusion is the dominant mechanism. The contribution to the spin-lattice relaxation of lattice phonons can be estimated from T_1 data on Br^{81} of Allen and Weber. It can be seen from Kocheleav's calculations[18] that

$$(T_1)_{\mathrm{phonon}} \propto m_0^2/\beta^2 Q^2,$$

where m_0 is the mass of the central ion, β is the effective antishielding factor, and Q is the quadrupole moment of the nucleus. With a value of 0.06 sec [7] for $(T_1^{\mathrm{Br}81})_{\mathrm{phonon}}$ at 300°K, one finds that $(T_1^{\mathrm{Li}7})_{\mathrm{phonon}}=131$ sec when $Q_{\mathrm{Br}}=0.28\times10^{-24}$ cm^2, $\beta_{\mathrm{Br}}=50$, $Q_{\mathrm{Li}^7}=5\times10^{-26}$ cm^2, and $\beta_{\mathrm{Li}^7}=0.74$ are used, while the largest experimental value for T_1 at 300°K was found to be 30 sec. The temperature dependence (T^{-2}) of the phonon contribution to spin-lattice relaxation of lithium, calculated from the data on Br^{81}, is shown in Fig. 4. It should, however, be noted that Allen and Weber's[7] work which extends to lower temperatures does not reveal any phonon contribution to spin-lattice relaxation of Li^7 in LiBr. So in this crystal, lattice vibrations make at most a small contribution to T_1 at the temperatures of interest here and can be neglected for all practical purposes. Allen and Weber found T_1^{Li} (300°K) to be about 200 sec, while the present value of 30 sec increases to about 140 after correcting for the difference in the frequencies of operation (they worked at 12 Mc/sec), assuming that the relaxation is due solely to diffusion. Both T_1 measurements, the present and those of Allen and Weber, exhibit qualitatively similar but quantitatively different behavior which is expected in the motionally narrowed region.

Reif's quadrupolar mechanism predicts a minimum in T_1 of about 7.3 sec for $c=5\times10^{-4}$ [cf. Eq. (2)] if $k'=0.3125$, corresponding to the vacancies restricted to sites of ions like the one undergoing relaxation, is used. With the vacancy jump frequency given to be[19] $\nu=5\times10^{13}\exp(-0.4/kT)$ Reif's theory predicts that this minimum should occur at about 350°K. Included in Fig. 4 in addition to the experimental data on sample B is the theoretical curve calculated according to the Reif mechanism for vacancy diffusion for $c_{\mathrm{ext}}=5\times10^{-4}$ per mole. Above about 350°K (i.e., above the minimum in T_1) the vacancy jump frequency is too high for the Reif process to be effective and thus the contribution of the Reif mechanism to spin-lattice relaxation of lithium at temperatures of interest here is negligible.

Another important mechanism which may contribute to relaxation is that of magnetic dipolar origin of the Torrey type discussed earlier. In the Reif mechanism vacancies diffuse with a jump frequency ν. But the rate of lithium-ion diffusion which is important in the dipolar mechanism is given by $cz\nu$ as seen earlier. Hence much higher temperatures are required before the lithium-ion jump frequency attains a value comparable to the Larmor frequency, the condition for a maximum in the transition probability. The temperature dependence of the relaxation time of lithium as expected from Torrey's theory for $c_{\mathrm{ext}}=5\times10^{-4}$ mole^{-1} is shown in Fig. 4. The calculations were made in the following way: First $y(T)$ was evaluated using 0.35 and 1.70 eV for the energy of migration of a vacancy and for creation of a Schottky-pair defect, respectively, as found in this investigation (see Table I). From these $y(T)$, $\psi(k,y)$ at different temperatures are obtained from the tables given by Resing

TABLE I. Activation energies.

Investigator	Technique	E_m (eV)	E_f (eV)
Ginnings and Phipps[a]	Ionic conductivity	0.56	1.32
Haven[b]	Ionic conductivity	0.39	1.80
Allen and Weber[c]	NMR	0.40	2.00
Present work	NMR	0.35	1.70

[a] D. C. Ginnings and T. E. Phipps, J. Am. Chem. Soc. **52**, 1340 (1930)
[b] See Ref. 19.
[c] See Ref. 7.

[18] B. I. Kocheleav, Zh. Eksperim. i Teor. Fiz. **37**, 242 (1959) [English transl.: Soviet Phys.—JETP **10**, 171 (1960)].

[19] Y. Haven, Rec. Trav. Chim. **69**, 1471 (1950).

and Torrey,[12] and $T_1(T)$ is then calculated using Eq. (1). We find a close agreement between these theoretical values and the experimental ones obtained on the sample B. In particular, we notice close coincidence at temperatures below T_1 minimum. In the intrinsic region, however, the experimental values are shifted relative to the theoretical ones by a constant factor. The reason for this probably lies in the preexponential factor c_0 in c_{int}. We used here a value of 820 for c_0 as obtained experimentally by Haven.[19] If this c_0 is multiplied by a constant factor, the $T_1(T)$ curve in the intrinsic region should be shifted relative to the one obtained with the original c_0. We can conclude from the above that the dominant relaxation mechanism is of the Torrey type with dipole-dipole interactions due to the diffusive motion of lithium ions. Further evidence for this conclusion is given below.

We note from the condition for the minimum in T_1, namely, $y=\omega_0/2\nu\approx 0.55$, that the temperature at which this minimum should occur T_c, is given by (here a value of 5×10^{13} sec^{-1} is used for ν_0 and this includes the number of nearest neighbors[19])

$$T_c \approx E_m/(14.28+\ln c)R\,, \tag{14}$$

where E_m is the energy of migration of a vacancy, c is the vacancy concentration, and R is the gas constant. It is clear from the above that as c increases, T_c should decrease. If then T_c falls in the extrinsic region, one expects to find this $T_{1\,\min}$ occuring at a lower temperature for higher concentration of divalent impurity ions and this is in harmony with the experimental results (see Fig. 5).

We now analyze the experimental data on different samples on T_1 as a function of temperature in the light of Torrey's theory. There are primarily three important regions to be considered depending on the temperature and the magnitude of ν_{Li} relative to the Larmor frequency: First, at low enough temperatures, $T_1 \propto 1/c\nu \sim e^{E_m/RT}$; second, in the region where $\nu_{\text{Li}} \gg \omega_0$ but still in the extrinsic region, $T_1 \propto c\nu \sim e^{-E_m/RT}$; and third, in the intrinsic region, $T_1 \propto c\nu \sim e^{-(\frac{1}{2}E_f+E_m)/RT}$. We should, however, note that if the Larmor frequency is high enough that the thermal vacancies come in before the condition $\omega_0 \approx \nu_{\text{Li}}$ is reached, then in the temperature region below T_1 minimum and in the intrinsic region, $T_1 \sim e^{+(\frac{1}{2}E_f+E_m)/RT}$, while in the region above T_c, $T_1 \sim e^{-(\frac{1}{2}E_f+E_m)/RT}$. The frequency of operation (5.5 Mc/sec) employed in this study is such that the earlier case is appropriate, while Allen and Weber used 12 Mc/sec, and they observed the latter situation.

It is possible to construct a universal curve using the table given by Resing and Torrey. Figure 5 shows overall plots of the temperature dependence of the normalized jump frequency $y(=\omega_0/2\nu_{\text{Li}})$, while the inset shows $T_1(T)$ for all four samples. The low-temperature y-versus-$1/kT$ curves for all the samples are roughly parallel and they yield an average value of 0.35 eV for

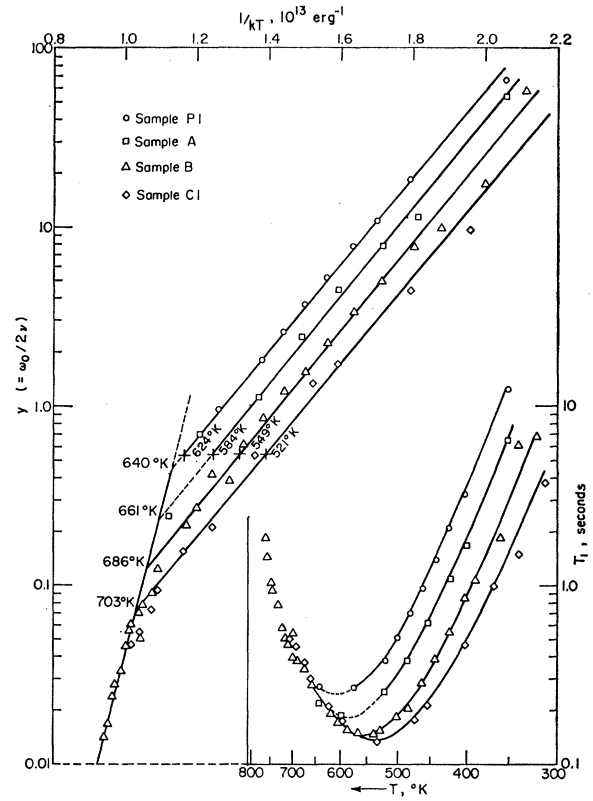

FIG. 5. Dependence of normalized jump frequency and spin-lattice relaxation time (inset) on temperature and concentration of divalent impurity.

the activation energy for migration of a vacancy. At high temperatures all four lines corresponding to the samples with different concentrations of Ca^{++} ions merge into a single line whose slope gives a value of 1.20 eV for $\frac{1}{2}E_f+E_m$, so that the energy of formation of a Schottky-pair defect is 1.70 eV. All these values are slightly smaller than, but comparable to, those obtained by ionic conductivity studies of Haven.

B. Pressure Dependence

From the previous analysis it is clear that below $T_{1\,\min}$, $T_1 \propto e^{E_m/RT}$, and above $T_{1\,\min}$, $T_1 \propto e^{-E_m/RT}$ at moderate temperatures, while $T_1 \propto e^{-(\frac{1}{2}E_f+E_m)/RT}$ at high temperatures. So far, the factor PV is neglected, and instead of the activation enthalpy H, only energies were considered. Now, to study the dependence of pressure it is important to add this relatively small term. Figure 6 shows the effect of pressure on the spin-lattice relaxation time for three samples. Since, as noted earlier, the thermo-emf of the thermocouples is a function of pressure, no isothermal data were obtained. Hence the lines connecting the data points are essentially isothermo-emf's. After correcting for this small effect on temperature, the data were analyzed and representative computer-smoothed isotherms were also shown in Fig. 6.

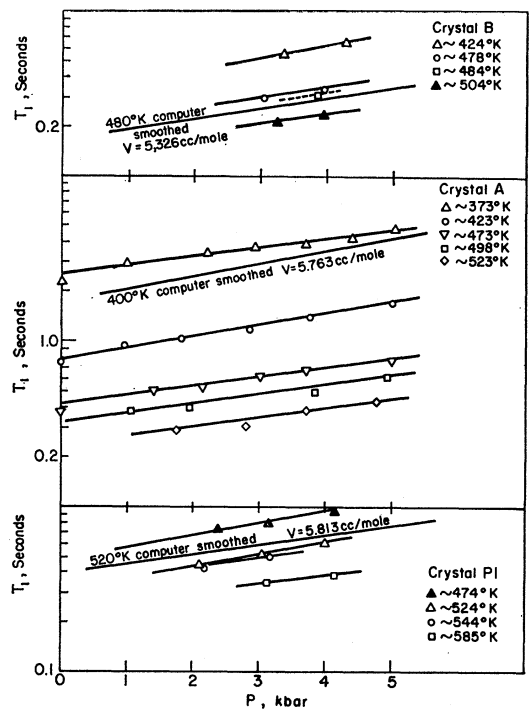

FIG. 6. Pressure dependence of T_1 under isothermo-emf conditions.

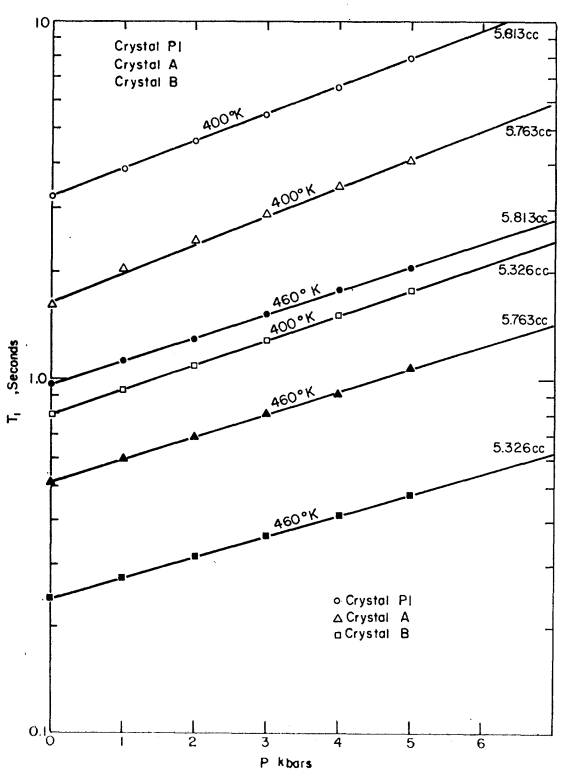

FIG. 7. Effect of pressure on T_1 at constant temperatures of 400 and 460°K.

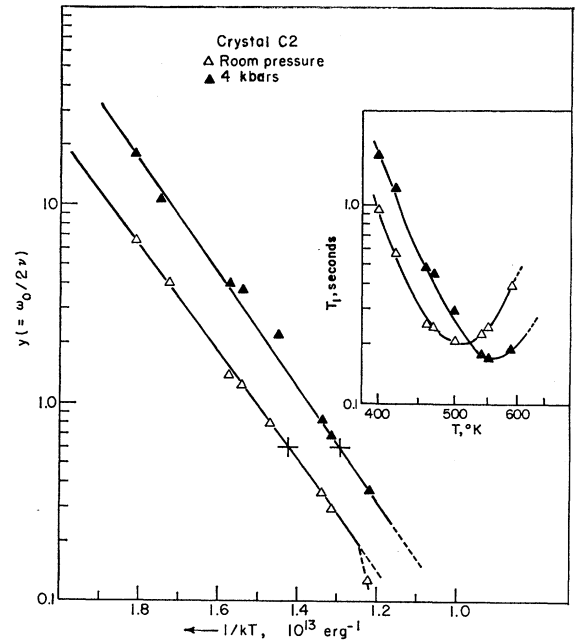

FIG. 8. Temperature dependence of normalized jump frequency and spin-lattice relaxation time (inset) at constant pressures of 4 kbar and room pressure.

The effect of pressure at constant temperature on T_1 of the three samples is shown in Fig. 7 and the indicated points were obtained from the computer output.

The transition through $T_{1\,\mathrm{min}}$ is well depicted in Fig. 8, where the inset shows $T_1(T)$ at room pressure and at a pressure of 4 kbar. These data in the inset were obtained from an extrapolation of the experimental determination of $T_1(P)$ at various temperatures. In the temperature region below T_c, T_1 increases with pressure, i.e., $T_1 \propto \nu^{-1} \sim e^{PV/RT}$, while above T_c, T_1 decreases with pressure, showing that $T_1 \propto \nu \sim e^{-PV/RT}$. We notice that $T_{1\,\mathrm{min}}$ decreases in value with pressure. Such a trend is expected since, with pressure, the lattice contracts, thereby increasing the transition probability, which is proportional to a^{-6}, where a is the nearest-neighbor distance. In addition to this shift in the magnitude of $T_{1\,\mathrm{min}}$, the pressure should increase T_c, the temperature at which this minimum occurs. This can be seen from the critical condition for the maximum in the transition probability:

$$\omega_0/2\nu \sim 0.55$$

or

$$\omega_0/2c\nu_0 \sim 0.55 e^{-(E_m+PV_m)/RT_c}.$$

So $T_c(P=0)$ should be smaller than T_c at finite pressure.

The effect of transition from extrinsic to intrinsic regions is clearly indicated in Fig. 9. As expected, T_1 decreases with pressure. The slopes of the straight lines at higher temperatures gave higher values for the activation volume which correspond to $\frac{1}{2}V_f + V_m$, where V_f and V_m are the volumes of creation of a Schottky pair and for the motion of a vacancy, respectively.

C. Activation Parameters

1. Activation Energies

Table I is a compilation of the activation energies obtained by previous investigators and by the present investigator. The value for the energy of migration of vacancies is found to be 0.35±0.01 eV, which is the average of the slopes of the four straight lines in Fig. 5. The high-temperature slope of ln$y$-versus-$1/kT$ graph yields a value of 1.20±0.02 eV, which fixes the value of energy of formation of a Schottky pair at 1.70 eV. The values obtained here are smaller than those of Haven, although in good agreement.

2. Activation Volumes

Activation volumes were evaluated using Eqs. (9), (11), and (12). Table II summarizes the data on activation volumes obtained on different samples. Pressure derivatives of spin-lattice relaxation time at constant temperature, obtained from the experimental data on $T_1(P)$, were found to be independent of temperature (in the extrinsic region) within experimental errors. Activation volumes thus obtained have to be corrected for the pressure dependence of the lattice parameter and the frequency factor ν_0 in the vacancy jump frequency. Equations (9) and (11) can be rewritten as

$$V_m = RT\left[\left(\frac{\partial \ln T_1}{\partial P}\right)_T + \beta(\gamma_G+2)\right], \quad T<T_c$$
$$= RT\left[-\left(\frac{\partial \ln T_1}{\partial P}\right)_T + \beta(\gamma_G-2)\right], \quad T>T_c \tag{15}$$

using

$$\beta = -3\frac{\partial \ln a}{\partial P} \quad \text{and} \quad \gamma_G = -\frac{\partial \ln \nu_0}{\partial \ln V},$$

where β is the isothermal compressibility and γ_G is the Grüneisen constant. We note that these equations are similar to those given by Hultsch and Barnes.[9] With $B=1/\beta=2.166\times10^{11}$ dyn/cm^2 and $\gamma_G=2.26$,[20] where B is the bulk modulus, we find that the corrections to be applied to the isothermal pressure derivatives of T_1 are

TABLE II. Activation volumes obtained from the pressure dependence of T_1.

Sample	Quantity measured[a]	$\pm RT(\partial \ln T_1/\partial P)_T$ [b] (cm^3/mole)	V (cm^3/mole)	Temperature region
$P1$	V_m	5.81±0.82	6.67±0.75	$T<T_c$
P2	V_m	5.63±0.56	6.44±0.59	$T<T_c$
$P2$	V_m	6.20±0.90	6.26±0.89	$T>T_c$
A	V_m	5.76±0.24	6.54±0.31	$T<T_c$
B	V_m	5.33±1.07	6.10±1.12	$T<T_c$
$P2$	$\frac{1}{2}V_f+V_m$	20.25±1.75	21.15±1.80	$T>T_c$

[a] $V_m=6.40$ cm^3/mole, $V_f=29.50$ cm^3/mole.
[b] + for $T<T_c$ and − for $T>T_c$.

[20] L. S. Ching, Ph.D. thesis, Cornell University, 1968 (unpublished).

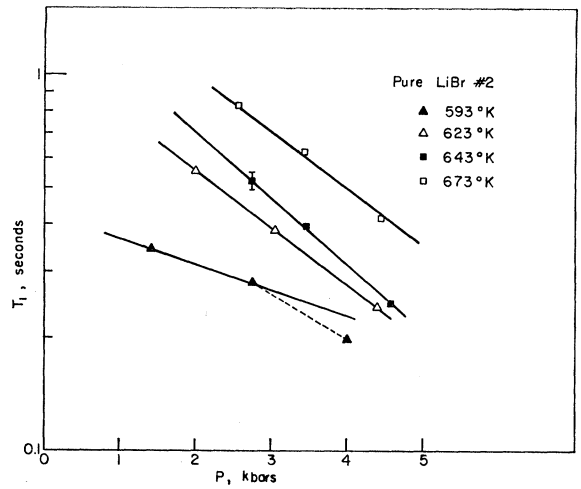

FIG. 9. T_1 as a function of pressure in the intrinsic region.

given (in cm^3/mole) by

$$\delta V_m = \beta(\gamma_G+2)RT = 16.35\times10^{-4}T, \quad T<T_c$$
$$= \beta(\gamma_G-2)RT = 1.00\times10^{-4}T, \quad T>T_c. \tag{16}$$

Included in Table II are the isothermal pressure derivatives, corrected activation volumes, and the temperature region. Thus the volumes of activation for migration of a vacancy and that for the creation of a Schottky pair are fixed to be 6.4 and 29.5 cm^3/mole, respectively. It is to be noted that the corrections δV_m were evaluated using Eq. (16) for temperatures uncorrected for the pressure dependence of emf of the thermocouples and this involves an error of less than 1%.

D. Miscellaneous Observations

In Sec. IV C 2 the activation volumes evaluated from the pressure dependence of spin-lattice relaxation time at constant temperature were presented. A further check can be made on this determination by plotting T_1 as a function of temperature at two different pressures. From these, the normalized jump frequency y can be evaluated as a function of temperature under isobaric conditions. Thus the plots of ln$k$ versus $1/kT$ at two different pressures should yield two slightly different enthalpies due to the difference in the relatively small term PV in the enthalpy. Figure 8 shows ln$y$ versus $1/kT$ at room pressure and at 4 kbar, calculated from $T_1(T)$ data shown in the inset. The two straight lines have slightly different slopes, which yield 0.356 and 0.383 eV for the enthalpy at room pressure and at 4 kbar, respectively. From these the migration volume of a vacancy is found to be 6.51 cm^3/mole, which is in excellent agreement with the previously obtained value. An estimate of this activation volume can be made from the values of T_c at room pressure and at 4 kbar. We note from the discussion of Sec. IVB that

$$(E_m+PV_m)/RT_c^P \approx E_m/RT_c,$$

TABLE III. Molar concentrations of cation vacancies calculated from T_c, T_c', and $\omega_0/2c\nu_0$ obtained from ln$y$-versus-$1/kT$ data (Fig. 5).

Crystal	T_c (°K)	$c(T_c)$[a] (mole^{-1})	T_c' (°K)	$c(T_c')$[b] (mole^{-1})	$\omega_0/2c\nu_0$	c (mole^{-1})	Doping c (mole^{-1})
$P1$	624±10	4.3×10^{-4}	640±10	1.7×10^{-4}	8.5×10^{-4}	4.1×10^{-4}	...
A	584	6.7×10^{-4}	661	2.7×10^{-4}	4.9×10^{-4}	7.1×10^{-4}	8.7×10^{-5}
B	549	1.0×10^{-3}	686	4.7×10^{-4}	3.1×10^{-4}	1.1×10^{-3}	4.4×10^{-4}
$C1$	521	1.6×10^{-3}	703	6.6×10^{-4}	2.4×10^{-4}	1.5×10^{-3}	2.2×10^{-3}
$C2$	510	1.8×10^{-3}	...	...	...	...	2.2×10^{-3}

[a] $c=2\pi10^{-7}\,e^{E_m/RT_c}$, $E_m=0.35$ eV.
[b] $c=820\,e^{-E_f/2RT_c'}$, $E_f=1.70$ eV.

Using $T_c^P\simeq560$°K at $P=4$ kbar and $T_c\simeq510$°K at room pressure, we calculate V_m to be 7.5 cm³/mole, which should be compared with 6.4 as obtained directly from the pressure dependence of T_1.

An interesting calculation can be made from the data in the inset of Fig. 8. We note that the two isobars cross each other at a temperature of about 525°K. We further notice that this T^0 is on the high-temperature side of T_c for the isobar at room pressure, while it lies on the low-temperature side of the 4-kbar isobar. So

$$T_1(T^0)=\tfrac{1}{2}Nc\nu_0a^6e^{-E/RT^0}$$
$$=[N2(a^P)^6\omega^2/c\nu_0{}^P]e^{(E+PV)/RT^0},$$

where the superscript P indicates that the correction for the pressure dependence has to be applied. From the above equality we find that

$$c=\frac{2\omega_0}{(\nu_0\nu_0{}^P)^{1/2}}\left(\frac{a^P}{a}\right)^3e^{(2E+PV)/2RT^0}.$$

$\nu_0{}^P$ and a^P can be written in the first approximation as

$$\nu_0{}^P=\nu_0+\left(\frac{\partial\nu_0}{\partial P}\right)P$$

and

$$a^P=a+\left(\frac{\partial a}{\partial P}\right)P.$$

Using

$$\frac{\partial\ln a}{\partial P}=-\tfrac{1}{3}\beta\quad\text{and}\quad\frac{\partial\ln\nu_0}{\partial P}=\gamma_G\beta,$$

we find that, for $\nu_0=5\times10^{13}$ sec^{-1}, $a=2.751$ Å, and $P=4$ kbar, $\nu_0{}^P=5.209\times10^{13}$ sec^{-1} and $a^P=2.734$ Å. With these values, the above expression for c yields a value of 5.2×10^{-3} per mole, which should be compared with 2.2×10^{-3}, corresponding to 0.5% $CaBr_2$ doping and 1.8×10^{-3}, estimated from $T_c=510$°K (see Table III). It should be noted, however, that the above calculations are valid for T^0 far from T_c, while here $T^0=525$°K is near to $T_c\sim510$°K. Hence the correspondence between the calculated value of c and the doping cannot be pushed any further than order-of-magnitude comparison.

An observation can be made from the data on the sample $P2$. By plotting T_1 versus $1/kT$ at constant pressures of room pressure and 4 kbar, the temperatures at which the transition from extrinsic to intrinsic regions occurs were found to be $T_c'(P=0)\sim575$°K and $T_c'(P=4$ kbar$)\sim620$°K. Since this transition is expected to occur when $c_{\text{doping}}=c_{\text{int}}$, one finds that

$$c_{\text{doping}}=c_0e^{-E_f/2R575}=c_0e^{-(E_f+PV_f)/2R620}.$$

With $E_f=1.70$ eV it is found that $PV_f=0.133$ eV at a pressure of 4 kbar. Converting this into cm³/mole, we find that $V_f=32.09$ cm³/mole, which compares reasonably with the previously obtained value of 29.5 cm³/mole for the formation volume of a Schottky pair.

We notice thus that knowledge of the transition temperatures T_c and T_c' should facilitate an estimation of the positive-ion vacancy concentration. The values of T_c, T_c' (see Figs. 5 and 8), concentration of Ca^{++} ions (doping), and c calculated both from T_c and T_c' are tabulated in Table III. From columns 3 and 4 of this table we note that $c(T_c)$ is about 2.4 times $c(T_c')$. In estimating c from T_c' we assumed a value of 820 for c_0 as obtained by Haven and this value may be in error. Also, T_c and T_c' can at best be estimated within ±10°K.

It should be noted, in addition, that the actual transition from extrinsic to intrinsic regions does not occur abruptly (see Fig. 5, where the experimental data smoothly change over from extrinsic to intrinsic regions, thereby deviating from the two straight lines near the transition). Thus the correct values of T_c at which c_{int} is exactly equal to c_{ext} should be greater than those listed in column 4 of Table III. This should explain why $c(T_c')$ as calculated above is smaller than $c(T_c)$.

The concentration c can be estimated in yet another way. In the extrinsic region

$$y=(\omega_0/2c\nu_0)e^{E_m/RT},$$

so that the preexponential term can be evaluated from y-versus-T data. The values of c obtained from these preexponential terms are in good agreement with those calculated from T_c (see Table III).

One more calculation may be of some interest to check the internal consistency of the calculation involved in the present study. From the temperature dependence of y, it is possible to evaluate c_0 assuming a value of 5×10^{13} sec^{-1} for ν_0. In the intrinsic region

$$y=(\omega_0/2c_0\nu_0)e^{(\frac{1}{2}E_f+E_m)/RT},$$

so that the least-squares analysis of ln$y$ versus $1/kT$ gives the value of the preexponential term. It is found

TABLE IV. Compilation of experimental and predicted values of activation volumes for various ionic crystals.

Material	Technique	Quantity measured	V_{expt} cm³/mole	V_{Keyes} (cm³/mole) Eq. (17)	Eq. (18)	Molar volume[a] cm³/mole	Reference
AgBr	Ionic cond.	V_m—Ag vac.	7.4	3.35	···	9 (Vol. Ag)	Kurnick[b]
	Ionic cond.	V_f—Schottky	~44	18	···	29 (Vol. AgBr)	Kurnick[b]
NaCl	Ionic cond.	V_m—Na vac.	7.7	9.1	6.6	5.4 (Vol. Na.)	Pierce[c]
KCl	Ionic cond.	V_m—K vac.	7.0	10.5	9.0	10.8 (Vol. K)	Pierce[c]
LiBr	NMR	V_m—Li vac.	6.4	6.0	5.8[d]	3.8 (Vol. Li)	This work
	NMR	V_f—Schottky	29.5	31.0	29.8[d]	25.1 (Vol. LiBr)	This work
	NMR	V_f+V_m—Li vac.	35.9	37.0	35.6[d]	25.1 (Vol. LiBr)	This work

[a] Approximate volume of the diffusing constituent.
[b] See S. W. Kurnick, J. Chem. Phys. 20, 219 (1952).
[c] See Ref. 23.
[d] With $C=1.236\times10^{11}$ dyn/cm² and $\partial C/\partial P=2.692$.

that

$$\omega_0/2c_0\nu_0=4.101\times10^{-10}.$$

c_0 can be calculated from the above to be 843, which compares with 820 of Haven.

V. DISCUSSION

It is clear, from the theoretical calculations based on the Reif and Torrey theories, and the experimental values of spin-lattice relaxation time as a function of temperature (see Fig. 4), that above about 350°K dipole-dipole interactions via the diffusive motion of lithium ions are mainly responsible for the spin-lattice relaxation of Li^7 in LiBr. An excellent agreement between the measured relaxation times and the calculated ones using Torrey's theory is found as in Fig. 4. However, it is to be borne in mind that in using the equation to obtain the relaxation times we have taken care of Li-Li dipolar interactions; but interactions of Li with Br also have to be accounted for. For Li-Br interactions k will be of the order of 0.5 and the effect of considering both Li-Li and Li-Br interactions does not change the calculated values for T_1 in any significant way except for a slight shift in the $T_{1\,\min}$. Even this shift in T_c is according to the estimates of Allen and Weber[7] comparable to the experimental uncertainties. Any change in $y(T_c)$ alters $c(T_c)$ and thus the values in column 3 of Table III. This might also be one of the reasons for a disagreement in $c(T_c)$ and $c(T_c')$ as calculated earlier.

The many areas of agreement between the experiment and theory notwithstanding, it is not clear why the minimum in T_1 is different for different crystals (see Fig. 5). For magnetic dipolar relaxation of Torrey type, T_1 is a function of c only through its dependence upon the lithium jump frequency $\nu_{Li}\approx cz\nu$. The minimum in T_1 occurs when $\omega_0\approx zc\nu$ and when this happens, ψ attains its maximum value of 0.4381,[12] and ψ_{max} is the same for any value of c. So there is no explicit c dependence in T_1 near its minimum. However, this kind of behavior is expected in Reif's mechanism, which, on the other hand, predicts no shift in T_c with c. But as already noted, Reif's mechanism predicts very long relaxation times above about 350°K. A similar controversy is found in Fig. 8. We have seen already that $T_{1\,\min}$(4 kbar) $<T_{1\,\min}$(room pressure). Using a(4 kbar) = 2.734 Å and a(room pressure) = 2.751 Å, we expect that $T_{1\,\min}$(4 kbar) should decrease by about 4%, while the experiment revealed a decrease of about 15%.

Table I reveals reasonable agreement between the values for energies obtained in the present investigation and those of Haven and of Allen and Weber. The activation volumes determined from the pressure dependence of the spin-lattice relaxation time are presented in Table II. Keyes[21] derived an expression relating the activation volume to the activation energy and the isothermal compressibility. His calculations were based on a strain-energy model where the work involved in creating or moving a defect is assumed to contribute entirely to the elastic strain energy. According to his model,[22]

$$V=\left[\left(\frac{\partial \ln C}{\partial P}\right)_T-\beta\right]G, \tag{17}$$

where C is the appropriate elastic shear modulus. Grüneisen's model of a solid simplifies the above expression to

$$V=2(\gamma_G-\tfrac{1}{3})\beta G, \tag{18}$$

where γ_G is the Grüneisen constant. The experimental measurements of activation volumes for various ionic crystals and the calculated values using Keyes's expression with the previously quoted values for γ_G and β are tabulated in Table IV. In the calculations on LiBr, we used the activation energy of 0.35 eV for the Gibbs free energy, assuming a negligible contribution of the term $PV-TS$ to the activation volume. Included in the above tabulation are the approximate volumes of the diffusing constituents. If the elastic constant data as a function of pressure are available, the activation volumes can be calculated from Eq. (17) without using Grüneisen's approximation. It may be of interest to note that the proper elastic constant that is of signifi-

[21] R. W. Keyes, J. Chem. Phys. 29, 467 (1958).
[22] R. W. Keyes, in *Solids Under Pressure*, edited by W. Paul and D. M. Warschauer (McGraw-Hill Book Co., New York, 1963).

cance here is[23]

$$C=\tfrac{3}{4}C_{44}+\tfrac{1}{5}(C_{11}-C_{12}).$$

We note a good agreement between the experimental values and those calculated from Keyes's model. The activation volume for migration of positive-ion vacancies in LiBr is smaller than that in either NaCl or KCl, as expected because of the comparatively smaller atomic volume of lithium.

It is noted from Table IV that V_m in ionic crystals is greater than the atomic volume available for the cation in the crystal lattice. Also, the results of the present experiments on LiBr and those of Kurnick on AgBr show clearly that V_f and V_t $(=V_f+V_m)$ are larger than the molar volume. On the other hand, the experiments of Hultsch and Barnes[9] and others[24] on metals indicate that volumes for self-diffusion (V_f+V_m) are considerably smaller than the atomic volumes. Aluminum is the only metal which seems to be an exception.[4] In metals such as copper considerable inward relaxation may occur about a vacancy as has been shown by Tewordt.[25] Pierce[23] observes that the large size of V_f in ionic crystals arises because the nearest neighbors of a given ion are repelled once it is removed from the original lattice site to form a vacancy. These Coulomb repulsions of ions are also probably responsible for the observation of large V_m in these crystals.

[23] C. B. Pierce, Phys. Rev. **123**, 744 (1961).
[24] D. Lazarus, in *Solids Under Pressure*, edited by W. Paul and D. M. Warschauer (McGraw-Hill Book Co., New York, 1963).

ACKNOWLEDGMENTS

The authors are grateful to Dr. G. W. Stupian for assistance in NMR experiments and for many suggestions. Thanks are due to Dr. P. G. McCormick for assistance in high-pressure experiments. Helpful discussions with Professor R. M. Cotts and efforts of G. E. Schmidt in growing the single crystals of LiBr are acknowledged.

[25] L. Tewordt, Phys. Rev. **99**, 61 (1958).

PHYSICAL REVIEW B VOLUME 1, NUMBER 1 1 JANUARY 1970

Charge-Transfer Spectra of Transition-Metal Ions in Corundum†

H. H. Tippins
Aerospace Corporation, El Segundo, California 90245
(Received 17 July 1969)

The ultraviolet absorption spectrum of corundum (Al_2O_3) containing dilute concentrations of the 3*d*-series transition-metal ions Ti^{3+}, V^{3+}, Cr^{3+}, Mn^{4+}, Fe^{3+}, and Ni^{3+} was measured at room temperature and at liquid-nitrogen temperature for photon energies in the range 3–9 eV. The most important features of the observed spectra are (a) the peak positions are characteristic of the particular impurity ion; (b) the peak positions and widths ($\sim$0.7 eV) are independent of temperature over the range studied; and (c) the integrated intensities are strong. The spectra are identified with the allowed transition whereby an electron is transferred from a nonbonding orbital, localized predominantly on the $O^{=}$ ligands, to either the $t_{2g}(\pi^*)$ or $e_g(\sigma^*)$ antibonding orbital, localized predominantly on the metal ion. The position in energy of the first absorption peak for the various ions of the series relative to one another and to the position of the intrinsic absorption edge of Al_2O_3 is in good agreement with the charge-transfer model.

I. INTRODUCTION

THE optical spectra of transition-group metal ions, present as substitutional impurities in ionic crystals, have been the subject of intense investigation in recent years.[1,2] These investigations have attempted to obtain a fundamental understanding of the varied colors and luminescent properties exhibited by the ions in different crystalline environments, and considerable progress has been made. However, with very few exceptions, the studies have been confined to spectra that arise as a result of transitions between energy levels internal to the substituted metal ion. These energy levels are those of the free ion modified by the intense crystalline electric fields of the host lattice. The present paper treats spectra that arise as a result of transitions between initial electronic states of the host crystal to final electronic states of the substitutional metal ion.

The absorption spectrum of a typical 3*d*-series ion at a concentration of about 10^{-2} mole % in Al_2O_3 shows several moderately strong absorption bands extending from the near infrared (IR) to the near uv, and then an abrupt intense cutoff at several eV on the low-energy side of the fundamental absorption edge of the host lattice (approximately 9 eV for Al_2O_3). The lower-energy transitions are the parity-forbidden transitions internal to the substituted ion, which have an oscillator strength

† This work was supported by the U. S. Air Force under Contract No. F04701-68-C-0200.
[1] D. S. McClure, Solid State Phys. **9**, 399 (1959).
[2] C. J. Ballhausen, *Introduction to Ligand Field Theory* (McGraw-Hill Book Co., New York, 1962).